

# Alignment or Integration? Rethinking Multimodal Fusion in DNA-language Foundation Models

Yanan Li<sup>1\*</sup>, Christina Yi Jin<sup>1\*</sup>, Yuan Jin<sup>1\*</sup>, Manli Luo<sup>1\*</sup>, Tie Xu<sup>1</sup>, Shuai Jiao<sup>2</sup>, Wei He<sup>1</sup>, Qing Zhang<sup>1†</sup>

<sup>1</sup>Research Center for Frontier Fundamental Studies, Zhejiang Lab

<sup>2</sup>Research Center for Scientific Data Hub, Zhejiang Lab

{liyn, cyj, jin.yuan, lml0502, fexutie, jiaoshuai, hewei, qing.zhang}@zhejianglab.org

## Abstract

Fusing DNA foundation models with large language models (LLMs) for DNA-language reasoning raises a fundamental question: at what level should genomic sequences and natural language interact? Most existing approaches encode DNA sequences and text separately and rely on embedding-level alignment to connect the two modalities. Such late-stage fusion compresses rich genomic sequences into fixed representations, limiting the model’s ability to reason over fine-grained, token-level genomic structure. In this work, we propose two new methods for DNA–language fusion, i.e. a semantic alignment method SeqCLIP and a vocabulary-level integration method OneVocab. SeqCLIP strengthens embedding-level alignment via sequence-level contrastive pre-training, and OneVocab directly integrates genomic  $k$ -mers into the language model’s existing vocabulary. Comprehensive experiments on classification and reasoning tasks show that, while various alignment strategies improve embedding-level fusion, early vocabulary-level integration yields more expressive and effective representations for DNA–language modeling.

## 1 Introduction

The field of artificial intelligence has been fundamentally reshaped by the rise of Transformer-based foundation models [Vaswani *et al.*, 2017; Naveed *et al.*, 2025; Pugliese *et al.*, 2025], most clearly seen in the success of Large Language Models (LLMs) such as ChatGPT [Schulman *et al.*, 2022]. Motivated by the observation that both DNA and natural language can be represented as discrete tokens with contextual dependencies, Transformer architectures originally developed for natural language processing have been repurposed to process genomic data. A series of DNA foundation models have been developed to understand complex genomic patterns at scale, such as DNABERT [Ji *et al.*, 2021], Nucleotide Transformer [Dalla-Torre *et al.*, 2025], Janus-DNA [Duan *et al.*, 2025], and Omnipreg-GPT [Wang *et al.*,

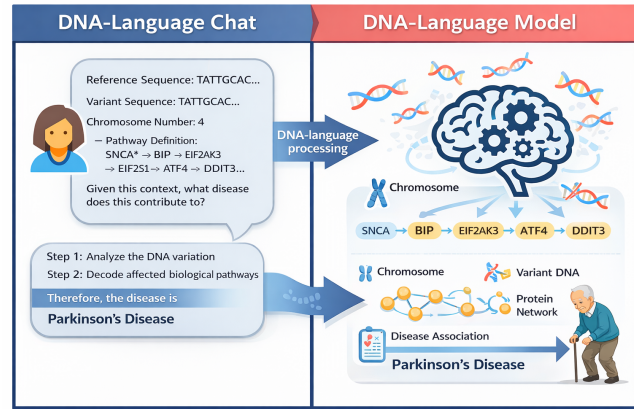


Figure 1: Illustration of the DNA-language reasoning task, where a DNA-language model reasons and produces a biologically meaningful answer to the textual query based on the given DNA sequences.

2025]. Pre-trained on large-scale genomic corpora, these models have shown reliable performance on a range of biological tasks, including promoter prediction, motif detection, and variant classification [Yang *et al.*, 2024; Refahi *et al.*, 2025].

However, existing DNA foundation models focus only on genomic sequences and cannot answer natural language queries about genomic data. Figure 1 illustrates the need for DNA–language models that jointly process genomic sequences and natural language inputs to enable end-to-end biological inference. Recent pioneer efforts toward DNA–language modeling have primarily adopted embedding-level alignment strategies [Fallahpour *et al.*, 2025; de Almeida *et al.*, 2025]. In these methods, latent representations are first extracted from genomic sequences using a pre-trained DNA encoder and are then mapped into the embedding space of a large language model via a learnable adapter. Such adapters are typically implemented as either simple linear projection or nonlinear, query-based projection.

Although adapter-based alignment is computationally convenient, it fundamentally limits how genomic information interacts with language models. In these methods, genomic sequences are first encoded independently and then mapped into the language model through embedding-level alignment.

\*Equal contribution. †: Corresponding author.

Consequently, the language model never reasons over genomic tokens or sequence structure, but only over their aggregated representations. This late-stage interaction restricts biological reasoning, as subtle but functionally important nucleotide variations, such as single-nucleotide polymorphisms (SNPs), maybe abstracted away during encoding. This limitation becomes more severe when aggressive compression is applied. For example, ChatNT [de Almeida *et al.*, 2025] compresses a 2048-token DNA sequence into 64 tokens before interacting with the language model, increasing the risk of losing fine-grained biological information.

These observations raise a fundamental question: at what level should genomic sequences and natural language interact? Beyond embedding-level alignment, is it possible to integrate genomic information directly at the vocabulary level, for example by including genomic tokens into the language model’s vocabulary to enable unified token-level interaction?

To answer this question, we revisit the current model fusion strategies and propose two novel methods: **SeqCLIP** and **OneVocab**. SeqCLIP extends existing adapter-based models by introducing an additional contrastive pre-training stage to strengthen embedding-level alignment between genomic sequences and biological textual descriptions. By explicitly enforcing cross-modal correspondence in the latent space, SeqCLIP enhances the effectiveness of alignment-based fusion without altering the underlying model architecture. OneVocab, a vocabulary-level integration approach, incorporates genomic  $k$ -mers directly into the vocabulary of LLMs. By treating genomic sequences as native linguistic tokens, OneVocab removes intermediate adapters and enables direct joint modeling of DNA and natural language within a unified token space.

To evaluate all these fusion strategies in DNA–language models, we conduct extensive experiments on classification and reasoning tasks. Classification tasks assess whether models can predict correct diseases, whereas reasoning tasks, still lacking systematic evaluation, examine the coherence and biological validity of multi-step inference processes. Our contributions are summarized as follows:

- We propose two novel DNA–language fusion methods: SeqCLIP, a semantic alignment-based approach, and OneVocab, a vocabulary integration-based approach.
- We develop an LLM-as-a-judge evaluation protocol to quantitatively assess DNA–language reasoning across multiple criteria: semantic similarity, logical coherence and completeness.
- We conduct extensive empirical studies on the NT [de Almeida *et al.*, 2025] and KEGG [Fallahpour *et al.*, 2025] benchmarks, covering both classification and reasoning tasks. The results consistently demonstrate the advantages of vocabulary-level integration for DNA–language modeling.

## 2 Related Work

### 2.1 Multimodal Fusion Paradigms in MLLMs

LLMs mainly perceive text. However, since the information in the real world is essentially multi-modal, bridging the

gap between natural language and other modalities is crucial to create systems with human-like understanding. The integration of external modalities has evolved into two primary paradigms based on the granularity of fusion, i.e., embedding-level alignment and vocabulary-level integration.

**Embedding-Level Alignment.** Current multimodal large language models (MLLMs) typically process separate modality information by the specific encoders, where textual inputs are represented discretely and non-textual signals are encoded into continuous representations that are subsequently aligned to the language model’s embedding space via learnable mappings [Zhang *et al.*, 2025]. Based on the complexity of the mapping interface, existing fusion strategies can be broadly categorized into three types:

(1) *Simple linear projection*: The most straightforward way to align non-textual features with an LLM’s embedding space is through a linear projection. Representative approaches employ one or two linear layers or shallow MLPs to match the dimensionality of non-textual tokens to that of word embeddings [Liu *et al.*, 2023; Zhang *et al.*, 2023b; Su *et al.*, 2023]. For instance, the LLaVA series [Liu *et al.*, 2023; Liu *et al.*, 2024] adopts lightweight linear projections to align visual features with textual embeddings. While computationally efficient, such linear mappings often lack sufficient capacity to bridge complex cross-modal semantic gaps.

(2) *Non-linear query-based projection*: To increase expressive power, a number of methods introduce learnable query tokens that extract modality-specific information in a query-driven manner. This paradigm was first popularized by BLIP-2 [Li *et al.*, 2023] and has since been adopted by many subsequent works [Zhang *et al.*, 2023a; Chen *et al.*, 2023]. For example, Flamingo [Alayrac *et al.*, 2022] employs a Perceiver Resampler to condense high-dimensional visual inputs into a fixed set of tokens, thereby reducing the computational cost of cross-modal attention while enabling more flexible non-linear alignment.

(3) *Explicit semantic alignment*: Beyond structural mappings, recent approaches further enhance fusion by explicitly aligning non-textual representations with textual semantics. In this setting, the adapter is encouraged to extract features that are directly informative for language modeling, rather than merely matching embedding dimensions. Owing to its strong semantic grounding, CLIP-style contrastive alignment has become a common choice in many MLLMs, including SigCLIP [Zhai *et al.*, 2023] and the InternViT series [Chen *et al.*, 2024].

**Vocabulary-Level Integration.** An alternative fusion paradigm moves beyond external encoders and adapter-based mappings by representing all modalities using discrete tokens within a unified vocabulary [Team, 2024; Sun *et al.*, 2023; Wang *et al.*, 2024]. In this setting, non-textual inputs such as images or videos are first quantized into sequences of discrete symbols, analogous to words in natural language, and are subsequently processed together with text tokens by a single transformer model. This approach enables cross-modal interaction from the earliest layers of the model, rather than postponing fusion to the embedding space. Prior studies have shown that with an effective tokenizer, vocabulary-level integration can achieve strong empirical performance across a

wide range of generation and perception tasks [Wang *et al.*, 2024].

## 2.2 DNA-Language Fusion Models

While general multimodal LLMs have explored a wide range of fusion strategies, from semantic alignment to unified tokenization, research on integrating genomic sequences with language models remains relatively limited. Most existing DNA-language models follow an alignment-based design, in which DNA sequences are first encoded by a specialized genomic model and then mapped into the language model’s representation space. For example, ChatNT [de Almeida *et al.*, 2025] combines a pre-trained DNA encoder (NTv2-500M) with Vicuna-7B through a query-based adapter, enabling language models to answer questions conditioned on genomic inputs. BioReason [Fallahpour *et al.*, 2025] adopts a simpler linear projection to align genomic representations with a large language model, and introduces a benchmark with step-by-step biological reasoning traces to evaluate model behavior under such alignment. In addition to alignment-based designs, Omni-DNA [Li *et al.*, 2025a] explores a vocabulary-level integration by starting from a pre-trained DNA foundation model and extending its vocabulary with a small set of trainable text tokens. However, the use of proprietary genomic components and undisclosed implementation details limits reproducibility and prevents systematic comparison under a unified experimental setting.

## 3 The Proposed Method

### 3.1 Problem Formulation

We formulated the task of DNA-language understanding as a cross-modal conditional generation task, which takes DNA sequences and English queries as input to produce an English answer as output. Formally, let  $S$  denote a DNA sequence with  $L$  nucleotide bases,  $Q$  denote the tokenized English query with  $N_q$  tokens (usually obtained by Byte-Pair Encoding (BPE) [Sennrich *et al.*, 2016]), and  $A = \{a_1, a_2, \dots, a_{N_a}\}$  denote the corresponding answer with  $N_a$  tokens. Our goal is to learn a DNA-language model  $f_\theta$  that can return a distribution  $p$  over English tokens that is used to autoregressively produce an answer in English, where  $\theta$  denotes the model parameters, i.e.

$$p(A|S, Q; \theta) = \prod_{k=1}^{N_a} p(a_k|S, Q, a_{<k}; \theta) \quad (1)$$

**The Status Quo.** Existing DNA-language models [Fallahpour *et al.*, 2025; de Almeida *et al.*, 2025] typically adopt the modular design, containing a DNA encoder  $f_{\text{DNA}}$ , an adapter  $g$ , and a LLM  $f_{\text{LLM}}$ , shown in Fig.2 (a). Specifically, the DNA encoder  $f_{\text{DNA}}$  maps the input sequence into contextualized embeddings, where  $S$  is first tokenized by a DNA-specific tokenizer and then mapped to a sequence of high-dimensional per-token embeddings. These embeddings are then mapped by the adapter  $g$  into the textual embedding space and concatenated with text token embeddings form the final input to the LLM. During model training, to ensure that

the model retains strong reasoning and text generation capabilities, we initialized with pre-trained encoders and LLMs, and then fine-tuned them in a parameter-efficient manner, e.g., LoRA, using the auto-regressive next-token prediction in the output sequence. Mathematically, we optimized the model by maximizing the log-likelihood of the observed sequences:

$$\mathcal{L} = \sum_i \log p(a_i|a_{<i}, S, Q; \theta), \quad (2)$$

where  $\theta$  denote the tunable parameters. For adapters, there are currently two main implementation paradigms in the literature:

- Linear mapping: DNA per-token embedding is projected by a learnable linear layer [Fallahpour *et al.*, 2025].
- Nonlinear mapping: DNA embeddings (e.g.,  $L$  tokens) are compressed into  $K$  query embeddings (e.g.,  $K = 64$  [de Almeida *et al.*, 2025]) by a nonlinear Q-former.

DNA sequences are characterized by exceptionally high information density, where a single nucleotide variation can potentially alter the function of an entire protein [Schiff *et al.*, 2024]. The above modular strategy that simply compresses genomic sequences into the textual embedding space may inevitably lead to irreversible information loss. For example, some seemingly minor nucleotide variations with substantial biological significance, e.g, Single Nucleotide Polymorphism (SNP), become indistinguishable in the embedding space. Furthermore, considering that LLMs are possibly rarely exposed to genomic vocabularies during pre-training, inferring gene functions through a simple adapter might not achieve true reasoning and primarily amounts to feature matching. We posit that a deeper fusion between genomic and textual modalities is required. This motivates us to systematically explore the following two extra paradigms that *remain underexplored in the field*.

### 3.2 SeqCLIP: Enhancing DNA-Language Alignment with Contrastive Learning

To alleviate the information loss issue inherent in the aforementioned modular strategy, a straightforward extension is to enhance the alignment between the gene encoded outcome and the textual embeddings at the pre-training stage, shown in Fig.2(b). Similar to recent progress in general MLLMs [Li *et al.*, 2023], we performed contrastive learning on the gene encoder  $f_{\text{DNA}}$  using large-scale paired gene-text data, thereby bootstrapping the adapter to extract representations that are most informative and semantically meaningful in the textual space.

SeqCLIP learns to align DNA representation and text representation such that their mutual information is maximized. To achieve so, it pulls together the embeddings of positive DNA-text pairs and pushes apart the embeddings for negative pairs. Let matrices  $\mathbf{D} = [D_1; D_2; \dots; D_M]$  and  $\mathbf{T} = [T_1; T_2; \dots; T_M]$  represent the batch of  $M$   $l_2$ -normalized embeddings of DNA and text modalities. Features in the same row are from the same positive pair, and features in different rows are from the negative pairs. The contrastive loss thus

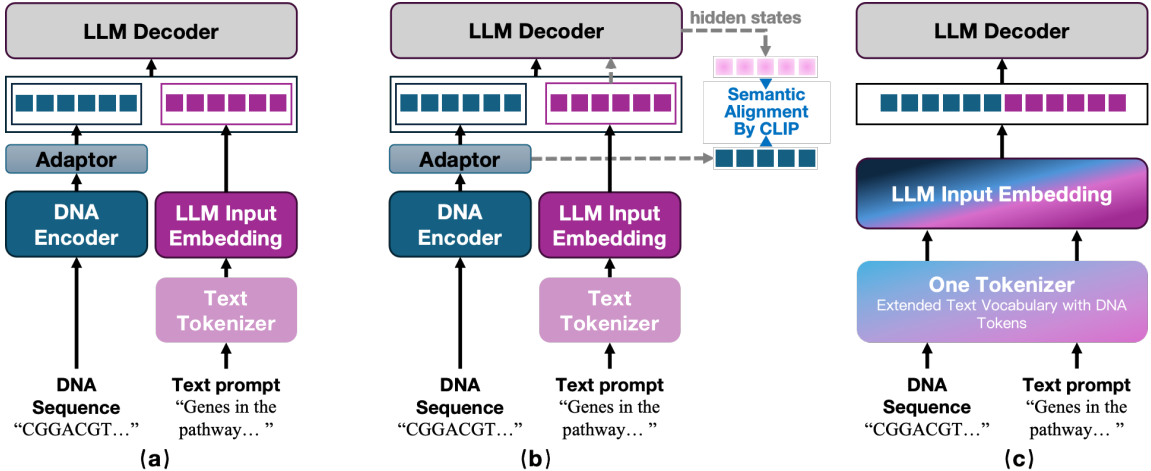


Figure 2: We systematically investigate three DNA-language fusion strategies, where the latter two are underexplored in the field. (a) The standard adapter-based architecture, adopted by current DNA-language models. (b) SeqCLIP: explicit semantic alignment on the gene encoder by contrastively learning on massive DNA-text pairs. (c) OneVocab: extend the pre-trained LLM’s vocabulary with DNA-specific tokens, allowing LLM to process them natively.

becomes:

$$\begin{aligned} \mathcal{L}_i^{d \rightarrow t} &= -\log \frac{\exp(D_i^\top T_i / \tau)}{\sum_{j=1}^M \exp(D_i^\top T_j / \tau)} \\ \mathcal{L}_i^{t \rightarrow d} &= -\log \frac{\exp(T_i^\top D_i / \tau)}{\sum_{j=1}^M \exp(T_i^\top D_j / \tau)} \\ \mathcal{L}_{\text{SeqCLIP}} &= \frac{1}{M} \sum_{i=1}^M (\mathcal{L}_i^{d \rightarrow t} + \mathcal{L}_i^{t \rightarrow d}) \end{aligned} \quad (3)$$

where  $\tau$  is a trainable temperature parameter initialized to 0.07 following [Radford *et al.*, 2021]. The text embedding  $T_i$  is the output embedding of the [CLS] token, while the DNA embedding  $D_i$  is the projected embedding after the adapter.

**Pre-trained DNA-text pairs.** We used the DNA-language dataset comprising 50,428 positive pairs from GeneChat [Dhanasekar *et al.*, 2025]. Each item includes a nucleotide sequence of the gene and its detailed textual description of its function. During training, we optimized both the DNA encoder and the adapter minimizing the loss function in Eq.3, while keeping the text encoder frozen.

CLIP-style pre-training enhances the alignment between global representations of DNA sequences and texts via a contrastive objective; however, it is inherently a coarse-grained alignment paradigm. In the context of genomic sequences, even a single nucleotide polymorphism (SNP) can fundamentally alter gene function. Such microscopic variations, constrained by the representational bottleneck of the adapter, are easily obscured under the global vector-level contrastive learning employed by CLIP. This observation naturally raises the question why the physical separation between modalities should be preserved at all. Instead, we present the following mechanism that allows native, fine-grained interactions between genomic sequences and text at the token level.

### 3.3 OneVocab: Vocabulary-Level Integration

Considering that genomic sequences share structural properties with natural language, an intuitive solution is to quantize the sequence into discrete tokens and let them share a unified processing paradigm. This can be achieved by extending the text vocabulary with a DNA vocabulary, i.e., OneVocab in Fig.2 (c). Compared with alignment in the embedding space, this approach is more native, as all scientific data are directly converted into a sequence of tokens and inferred within a single, unified embedding space.

Let  $V_t$  denote the original text vocabulary in LLMs, and  $V_d$  denote the DNA vocabulary. The new vocabulary is defined as  $V = V_t \cup V_d$  with size  $|V| = |V_t| + |V_d|$ . The embedding layer in LLM now changes from  $\mathbf{E} \in \mathbb{R}^{|V_t| \times d}$  to  $\mathbf{E}_{\text{new}} \in \mathbb{R}^{|V| \times d}$ . The initial hidden state  $\mathbf{H}^0$  is then constructed by concatenating the embeddings of the DNA sequence  $S$  and the text query  $Q$ :

$$\mathbf{H}^0 = [LN(\mathbf{E}_{\text{new}}(S) + \mathbf{P}_s), LN(\mathbf{E}_{\text{new}}(Q) + \mathbf{P}_q)] \quad (4)$$

where  $LN(\cdot)$  denotes the Layer Normalization, while  $\mathbf{P}_s$  and  $\mathbf{P}_q$  are the positional embeddings for the DNA and text sequences, respectively. The transformer’s self-attention mechanism can compute the interaction weight  $\alpha_{ij}$  between genomic and textual tokens in a lossless manner:

$$\alpha_{ij} = \frac{\exp(e_{ij})}{\sum_k \exp(e_{ik})}, e_{ij} = \frac{(\mathbf{h}_i \mathbf{W}^Q)(\mathbf{h}_j \mathbf{W}^K)^\top}{\sqrt{d}} \quad (5)$$

where  $d$  is the scaling factor. When  $\mathbf{h}_i$  denotes the  $i$ -th text token and  $\mathbf{h}_j$  denotes the  $j$ -th DNA token, the attention weight directly characterizes the model’s focus on specific biological sequence segments during the generative process, thereby avoiding the information filtering encountered in the adapter architectures. The probability of generating token  $a_t$  is given by the softmax in Eq.2:

$$p(a_t | a_{<t}, S, Q) = \frac{\exp(h_{t-1}^\top e_{a_t})}{\sum_{i=1}^{|V|} \exp(h_{t-1}^\top e_{a_i})} \quad (6)$$

where  $h_{t-1}$  is the last hidden state of the decoder at step  $t-1$ . The matrix  $E = [e_v]_{v \in V} \in \mathbb{R}^{d \times |V|}$  is the output embedding matrix, where each column vector  $e_v$  corresponds to the representation of a token in the joint vocabulary  $V$ .

## 4 Experiments

### 4.1 Experimental Settings

**Datasets.** Following [Fallahpour *et al.*, 2025; de Almeida *et al.*, 2025], we evaluated our methods on two downstream tasks (i.e., classification and reasoning) with two widely adopted benchmarks, the Nucleotide Transformer Benchmark (NT) [de Almeida *et al.*, 2025] and the KEGG-Derived Biological Reasoning Dataset (KEGG) [Fallahpour *et al.*, 2025]. The NT benchmark consists of relative simple question-answer pairs, where each instance contains one or two DNA sequences together with a natural language question. The KEGG benchmark focuses on biological reasoning rather than a simple choice, requiring the models to be able to reason biologically before generating the final answer. For both benchmarks, we adopted the same training, validation, and test splits as in [Fallahpour *et al.*, 2025; de Almeida *et al.*, 2025]. Additional details and results are provided in the supplementary material due to space constraints.

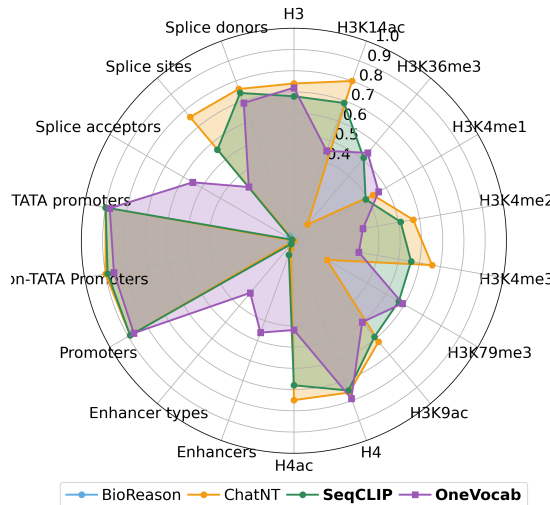


Figure 3: MCC on the 18 tasks in NT. Our model achieves superior performance compared with others on the vast majority of tasks, while exhibiting more balanced performance across tasks.

**Evaluation metrics.** We adopted task-specific evaluation metrics. For NT, following [Schiff *et al.*, 2024; de Almeida *et al.*, 2025; Li *et al.*, 2025b], we reported Mathews Correlation Coefficient (MCC). For the remaining classification settings, we used accuracy, macro F1-score, macro precision and macro recall. To evaluate the reasoning capability, we further developed an LLM-as-a-judge protocol that compares model outputs with the ground truth reasoning along three dimensions: *semantic similarity*, *logical coherence*, and

*completeness*. Each dimension is scored on a 0 – 10 scale, where higher scores indicate better reasoning quality.

- *Semantic similarity* assesses whether the predicted reasoning matches the ground truth in terms of biological concepts, molecular mechanism descriptions, and domain-specific terminology.
- *Logical coherence* evaluates the consistency and soundness of the reasoning process, including the validity of step-to-step transitions, clarity of causal relations, and the absence of contradictions or unjustified leaps.
- *Completeness* measures whether the reasoning covers the necessary steps and key elements required to support the final answer, without missing critical components.

We used dedicated prompts for each dimension (see the supplement) and employ OpenAI’s o3-mini to generate the scores.

**Implementation details.** Qwen3-1.7B [Yang *et al.*, 2025] was used as the language model backbone, and a 6-mer tokenizer is adopted for DNA sequence encoding. All experiments were conducted on 8 NVIDIA A100 GPUs. Models are optimized using the Adam optimizer with  $\beta_1 = 0.9$ ,  $\beta_2 = 0.999$ , a weight decay of 0.05, and a learning rate of  $10^{-6}$ . For SeqCLIP, LoRA fine-tuning was applied following [Fallahpour *et al.*, 2025], with the rank set to 8. The batch size was set to 1, and gradients were accumulated over 8 steps. For OneVocab, the entire model was optimized by default.

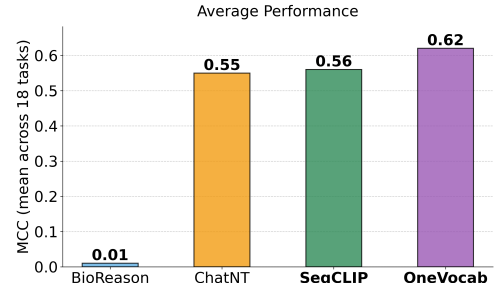


Figure 4: Average MCC across 18 NT tasks. Our two methods achieves the best.

### 4.2 Comparison with State-of-the-Arts

**Classification task.** We report results on the 18 NT tasks in Fig. 3, with average performance shown in Fig. 4. Classification results on KEGG are summarized in Tab. 1, with additional details provided in the supplementary material. Overall, three observations can be made: (1) SeqCLIP consistently outperforms BioReason, demonstrating that introducing explicit CLIP-style semantic alignment substantially improves adapter-based models. (2) OneVocab achieves the strongest and most balanced performance across all 18 NT tasks. (3) On the more challenging KEGG benchmark with 37 disease classes, OneVocab attains a state-of-the-art accuracy of 99.31%, significantly outperforming BioReason and ChatNT. Notably, comparison between BioReason and SeqCLIP reveals a clear precision-recall trade-off: while BioReason attains higher accuracy, SeqCLIP achieves a substantially higher macro-F1 score (90.31 vs. 72.13), suggesting

<b>DNA</b>	Reference sequence: TTTAAAAATACATAC <b>AGAAAAAGACGTTTGGACTTAAATCCTCTTC...</b> Variant sequence: TTTAAAAATACATAC <b>G</b> AAAAAGACGTTTGGACTTAAATCCTCTTC...
<b>Question</b>	Chromosome Number: 19 Network Definition of the pathway: Ca2+(extracellular) // CACNA1A* // Ca2+ Genes in the pathway: CACNA1A; calcium voltage-gated channel subunit alpha1 A Given this context, what is the biological effect of this CACNA1A allele, specifically what disease does this contribute to?
<b>Ground Truth</b>	Step 1: The A>G substitution at position 13303579 on chromosome 19 occurs in the CACNA1A gene, which encodes the alpha-1A subunit of P/Q-type voltage-gated calcium channels..... This A>G mutation in CACNA1A likely alters the function of the P/Q-type calcium channel, affecting calcium influx in cerebellar neurons. The resulting disruption in calcium homeostasis contributes to <b>spinocerebellar ataxia (SCA6)</b> characterized by progressive cerebellar degeneration, balance problems, and motor incoordination.
	Step 1: The variant is a deletion of 2 nucleotides (TT) at position 148688093 on chromosome 19, affecting the CACNA1A gene..... This CACNA1A deletion variant likely disrupts the function of the calcium voltage-gated channel, altering calcium homeostasis in cerebellar neurons. This dysregulation contributes to spinocerebellar ataxia type 6 (SCA6), characterized by progressive cerebellar degeneration, balance problems, and motor incoordination.
	Step 1: The variant KEGG_358 is an A>T substitution at position 2460579 on chromosome 19, which corresponds to the CACNA1A gene..... This A>T mutation in CACNA1A likely results in dysfunctional L-type voltage-gated Ca <sup>2+</sup> channels, disrupting normal myocardial and vascular calcium signaling. The genetic defect contributes to hypertension by impairing vascular smooth muscle relaxation and increasing vascular resistance.
	Step 1: The variant KEGG_752 is a C>T substitution at position 13304489 on chromosome 19, occurring in the CACNA1A gene..... This C>A>G>C mutation in the CACNA1A gene likely alters the function of the calcium voltage-gated channel, disrupting calcium homeostasis in cerebellar neurons. This dysregulation contributes to Spinocerebellar Ataxia type 14 (SCA14), an autosomal dominant neurodegenerative disorder characterized by progressive loss of balance and motor coordination due to cerebellar dysfunction.
	Answer: spinocerebellar ataxia type 6
<b>BioReason</b>	<b>3.0, 5.0, 4.0</b>
<b>ChatNT</b>	<b>2.0, 3.0, 2.5</b>
<b>SeqCLIP</b>	<b>4.0, 7.0, 5.0</b>
<b>OneVocab</b>	<b>8.0, 9.0, 8.5</b>

Figure 5: One KEGG reasoning case study (full reasoning steps are provided in the supplement). The red box indicates the ground truth disease; red text marks incorrect answers, and the numbers after each method denote the semantic, logical, and completeness score.

that explicit semantic alignment helps reduce false positives by grounding genomic features in biological descriptions.

Method	Accuracy	F1-score	Precision	Recall
BioReason	88.42	72.13	75.42	71.91
ChatNT*	46.94	17.58	21.42	15.85
SeqCLIP	87.50	90.31	94.44	87.50
<b>OneVocab</b>	<b>99.31</b>	<b>95.24</b>	<b>96.43</b>	<b>94.64</b>

Table 1: Classification performance comparison on KEGG. The superscript \* means that we re-implement ChatNT by replacing the pre-trained Vicuna-7B with the same Qwen3-1.7B as others. Our OneVocab achieves the best on all metrics.

**Reasoning task.** We evaluated reasoning performance using the proposed LLM-as-a-judge protocol, with results summarized in Tab. 3. Several observations can be drawn: (1) ChatNT, compressing DNA sequences into a fixed set of 64 tokens, exhibits the weakest performance in reasoning. This supports the hypothesis that embedding-level fusion with aggressive compression can lead to irreversible information loss, making fine-grained genomic signals difficult to preserve in the textual embedding space. (2) SeqCLIP outperforms ChatNT despite using a simpler linear mapping, suggesting that explicit semantic alignment benefits the genomic–textual reasoning. (3) OneVocab consistently achieves the best on all evaluation dimensions, indicating that native tokenization of DNA sequences enables the language model to move beyond superficial pattern matching toward a deeper understanding of biological information.

Fig.5 presents an *example* comparing the reasoning output using different methods querying about the biological effect of a CACNA1A allele on Chromosome 19, given its associated pathway information. It reveals different failure modes based on our evaluation criteria. BioReason identifies the correct disease, but its explanation mainly relies on gene–disease

associations, with limited semantic detail and little mechanistic support. This results in lower scores in semantic similarity and completeness despite relatively fine logical consistency. ChatNT shows a more fundamental failure: it misidentifies the biological role of the target gene, which leads to domain-inconsistent reasoning across steps and ultimately generates an incorrect disease prediction, although the overall reasoning appears fluent. SeqCLIP produces long, step-by-step explanations with relatively coherent narratives; however, incorrect disease attribution and unsupported mechanistic assumptions significantly reduce its semantic alignment to the ground truth reasoning and its overall completeness. OneVocab operates directly on constructing biologically meaningful tokens, rather than relying on late-stage embedding alignment. Such an early-stage integration allows the model to follow coherent biological reasoning paths from molecular function to cellular context and disease phenotype, instead of handling these aspects as loosely related signals. Accordingly, OneVocab demonstrates strong and balanced performance on all three evaluation criteria.

### 4.3 Ablation Studies

**Fine-tuning strategies for OneVocab.** To understand how different fine-tuning strategies influence vocabulary-level integration, we performed ablations on KEGG by selectively training or freezing different model parts. As shown in Tab. 2, we considered three settings: (i) fine-tuning the LLM backbone together with extended *DNA* token embeddings, (ii) fine-tuning the backbone with *text* token embeddings but freezing the *DNA* token embeddings, leaving them at their parameter initialization state, and (iii) jointly fine-tuning both the backbone and all embeddings. The results show that tuning *DNA* embeddings (Row 1) leads to higher performance than tuning *text* embeddings (Row 2), scoring higher on both classification and reasoning metrics, suggesting that adapting

DNA Embeds	Text Embeds	Backbone	Classification					Reasoning	
			Acc	F1	Precision	Recall	Semantic	Logical	Completeness
✓	✗	✓	97.92	92.67	92.86	92.50	8.43	8.80	8.59
✗	✓	✓	86.81	75.70	74.85	77.68	6.93	7.79	7.29
✓	✓	✓	<b>99.31</b>	<b>95.24</b>	<b>96.43</b>	<b>94.64</b>	<b>8.46</b>	<b>8.85</b>	<b>8.64</b>

Table 2: Impact of fine-tuning different modules on KEGG. ✗ and ✓ denote frozen and fine-tuning, respectively.

Method	Semantic	Logical	Completeness
BioReason	4.89	6.11	5.41
ChatNT*	4.89	5.68	5.20
<b>SeqCLIP</b>	7.17	7.99	7.52
<b>OneVocab</b>	<b>8.46</b>	<b>8.85</b>	<b>8.64</b>

Table 3: Reasoning performance on KEGG, assessed using our proposed LLM-as-a-judge strategy. We used OpenAI’s o3-mini to generate the reasoning scores. The superscript \* means that we re-implemented ChatNT by replacing the Vicuna-7B LLM with the same Qwen3-1.7B as other comparison models.

$k$	Voc Size	Seq	Acc	F1	MCC	tt (s)
7	78,125	200	0.75	0.74	0.53	1688
6	15,625	200	<b>0.80</b>	<b>0.78</b>	<b>0.62</b>	<b>521</b>
4	625	280	0.80	0.78	0.61	725
3	125	330	0.80	0.79	0.62	841
2	25	420	0.79	0.77	0.61	1074
1	5	720	0.76	0.73	0.54	4597

Table 4: Impact of  $k$  in  $k$ -mer tokenization of DNA sequences on NT classification task. “Voc Size”, “Seq” and “tt” are short for vocabulary size, sequence length, and training time, respectively.

genomic tokens is critical to not only pathway prediction but also downstream biological reasoning. Jointly tuning both the DNA and text embeddings together with the backbone (Row 3) achieves the most balanced and highest performance.

**Effect of the  $k$ -mer vocabulary size.** We examined the impact of  $k$ -mer tokenization (Tab. 4). Model training time exhibits a non-monotonic trend, reaching its minimum at  $k = 6$ , and increases noticeably at  $k = 7$ . Very small  $k$  values fail to capture biologically meaningful patterns, shown as decreased task performance, while excessively large  $k$  dramatically expands the vocabulary size, leading to data sparsity and increased optimization difficulty. Intermediate  $k$  values (e.g.,  $k = 6$ ) strike a balance between expressiveness and tractability.

#### 4.4 Probing the Latent Space

To elucidate the internal mechanisms of different fusion strategies, UMAP [McInnes *et al.*, 2018] is used to visualize the distributions of gene and text embeddings before they enter the LLM decoder (Fig.6). The embedding distribution exhibits structural diversity across strategies. Linear alignment (BioReason) results in substantial overlap between the gene and text modalities, while non-linear alignment (ChatNT) yields two largely juxtaposed manifolds with a clear separation, indicating its limited cross-modal information fusion. Semantic alignment (SeqCLIP) yields an asymmetric embedding geometry dominated by one modality, suggesting imbalanced information contribution from modalities. Finally, vo-

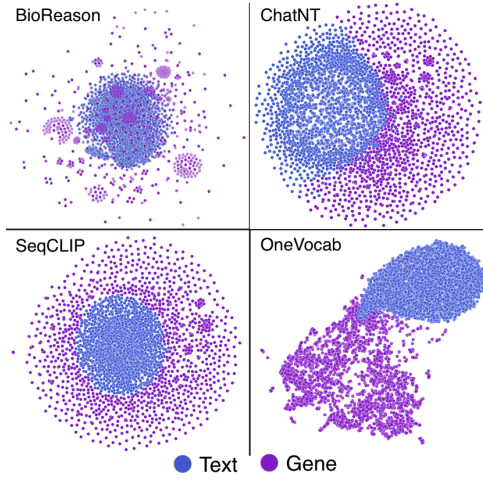


Figure 6: UMAP visualizations of gene and text embeddings across different methods on KEGG.

cabulary integration (OneVocab) forms a unified embedding space in which gene and text representations are genuinely integrated.

These structural diversity in the embedding space provides a geometric explanation for the observed downstream task performance. Overlap between the text and DNA embeddings as observed from the linear-alignment-based models may obscure modality-specific information. Juxtaposed or imbalanced structure of the embeddings space limits effective cross-modal interaction and leads to reduced reasoning capability. In contrast, the unified embedding space derived from the vocabulary-level integration enables both the information sharing and structural diversity, and thus benefits the superior performance on downstream tasks.

## 5 Conclusion

We revisit DNA-language modeling from the perspective of interaction granularity between genomic sequences and natural language, systematically comparing embedding-level alignment and vocabulary-level integration. Our analysis reveals fundamental limitations of late-stage fusion at the embedding level, particularly under aggressive compression and isolated modality processing. In contrast, vocabulary-level integration provides a more expressive and robust foundation for both classification and biological reasoning. By treating genomic sequences as native tokens, this paradigm preserves fine-grained genomic information and enables more faithful multi-step inference, suggesting a promising direction for future DNA–language foundation models beyond purely alignment-based fusion.

## References

[Alayrac *et al.*, 2022] Jean-Baptiste Alayrac, Jeff Donahue, Pauline Luc, Antoine Miech, Iain Barr, Yana Hasson, Karel Lenc, Arthur Mensch, Katherine Millican, Malcolm Reynolds, et al. Flamingo: a visual language model for few-shot learning. *Advances in neural information processing systems*, 35:23716–23736, 2022.

[Chen *et al.*, 2023] Feilong Chen, Minglun Han, Haozhi Zhao, Qingyang Zhang, Jing Shi, Shuang Xu, and Bo Xu. X-llm: Bootstrapping advanced large language models by treating multi-modalities as foreign languages. *arXiv preprint arXiv:2305.04160*, 2023.

[Chen *et al.*, 2024] Zhe Chen, Jiannan Wu, Wenhui Wang, Weijie Su, Guo Chen, Sen Xing, Muyan Zhong, Qinglong Zhang, Xizhou Zhu, Lewei Lu, et al. Internvl: Scaling up vision foundation models and aligning for generic visual-linguistic tasks. In *Proceedings of the IEEE/CVF conference on computer vision and pattern recognition*, pages 24185–24198, 2024.

[Dalla-Torre *et al.*, 2025] Hugo Dalla-Torre, Liam Gonzalez, Javier Mendoza-Revilla, Nicolas Lopez Carranza, Adam Henryk Grzywaczewski, Francesco Oteri, Christian Dallago, Evan Trop, Bernardo P de Almeida, Hassan Sirekhathim, et al. Nucleotide transformer: building and evaluating robust foundation models for human genomics. *Nature Methods*, 22(2):287–297, 2025.

[de Almeida *et al.*, 2025] Bernardo P de Almeida, Guillaume Richard, Hugo Dalla-Torre, Christopher Blum, Lorenz Hexemer, Priyanka Pandey, Stefan Laurent, Chandana Rajesh, Marie Lopez, Alexandre Laterre, et al. A multimodal conversational agent for dna, rna and protein tasks. *Nature Machine Intelligence*, pages 1–14, 2025.

[Dhanasekar *et al.*, 2025] Shashi Dhanasekar, Akash Saranathan, and Pengtao Xie. Genechat: A multi-modal large language model for gene function prediction. *bioRxiv*, pages 2025–06, 2025.

[Duan *et al.*, 2025] Qihao Duan, Bingding Huang, Zhenqiao Song, Irina Lehmann, Lei Gu, Roland Eils, and Benjamin Wild. Janusdn: A powerful bi-directional hybrid dna foundation model. *arXiv preprint arXiv:2505.17257*, 2025.

[Fallahpour *et al.*, 2025] Adibvafa Fallahpour, Andrew Magnuson, Purav Gupta, Shihao Ma, Jack Naimer, Arnav Shah, Haonan Duan, Omar Ibrahim, Hani Goodarzi, Chris J Maddison, et al. Bioreason: Incentivizing multi-modal biological reasoning within a dna-llm model. *arXiv preprint arXiv:2505.23579*, 2025.

[Ji *et al.*, 2021] Yanrong Ji, Zhihan Zhou, Han Liu, and Rama V Davuluri. Dnabert: pre-trained bidirectional encoder representations from transformers model for dna-language in genome. *Bioinformatics*, 37(15):2112–2120, 2021.

[Li *et al.*, 2023] Junnan Li, Dongxu Li, Silvio Savarese, and Steven Hoi. Blip-2: Bootstrapping language-image pre-training with frozen image encoders and large language models. In *International conference on machine learning*, pages 19730–19742. PMLR, 2023.

[Li *et al.*, 2025a] Zehui Li, Vallijah Subasri, Yifei Shen, Dongsheng Li, Wentao Gu, Guy-Bart Stan, Yiren Zhao, and Caihua Shan. Omni-dna: A genomic model supporting sequence understanding, long-context, and textual annotation. In *Advances in Neural Information Processing Systems*, 2025.

[Li *et al.*, 2025b] Zehui Li, Vallijah Subasri, Yifei Shen, Dongsheng Li, Wentao Gu, Guy-Bart Stan, Yiren Zhao, and Caihua Shan. Omni-dna: A genomic model supporting sequence understanding, long-context, and textual annotation. In *The Thirty-ninth Annual Conference on Neural Information Processing Systems*, 2025.

[Liu *et al.*, 2023] Haotian Liu, Chunyuan Li, Qingyang Wu, and Yong Jae Lee. Visual instruction tuning. *Advances in neural information processing systems*, 36:34892–34916, 2023.

[Liu *et al.*, 2024] Haotian Liu, Chunyuan Li, Yuheng Li, and Yong Jae Lee. Improved baselines with visual instruction tuning. In *Proceedings of the IEEE/CVF conference on computer vision and pattern recognition*, pages 26296–26306, 2024.

[McInnes *et al.*, 2018] Leland McInnes, John Healy, and James Melville. Umap: Uniform manifold approximation and projection for dimension reduction. *arXiv preprint arXiv:1802.03426*, 2018.

[Naveed *et al.*, 2025] Humza Naveed, Asad Ullah Khan, Shi Qiu, Muhammad Saqib, Saeed Anwar, Muhammad Usman, Naveed Akhtar, Nick Barnes, and Ajmal Mian. A comprehensive overview of large language models. *ACM Transactions on Intelligent Systems and Technology*, 16(5):1–72, 2025.

[Pugliese *et al.*, 2025] Raffaele Pugliese, Silvia Badini, Emanuele Frontoni, and Stefano Regondi. Generative artificial intelligence for advancing discovery and design in biomateromics. *Intelligent Computing*, 4:0117, 2025.

[Radford *et al.*, 2021] Alec Radford, Jong Wook Kim, Chris Hallacy, Aditya Ramesh, Gabriel Goh, Sandhini Agarwal, Girish Sastry, Amanda Askell, Pamela Mishkin, Jack Clark, et al. Learning transferable visual models from natural language supervision. In *International conference on machine learning*, pages 8748–8763. PMLR, 2021.

[Refahi *et al.*, 2025] Mohammadsaleh Refahi, Mahdi Abavizani, Bahrad A Sokhansanj, James R Brown, and Gail Rosen. Context-aware regularization with markovian integration for attention-based nucleotide analysis. *arXiv preprint arXiv:2507.09378*, 2025.

[Schiff *et al.*, 2024] Yair Schiff, Chia-Hsiang Kao, Aaron Gokaslan, Tri Dao, Albert Gu, and Volodymyr Kuleshov. Caduceus: Bi-directional equivariant long-range dna sequence modeling. *Proceedings of machine learning research*, 235:43632, 2024.

[Schulman *et al.*, 2022] John Schulman, Barret Zoph, Christina Kim, Jacob Hilton, Jacob Menick, Jiayi Weng,

Juan Felipe Ceron Uribe, Liam Fedus, Luke Metz, Michael Pokorny, et al. Chatgpt: Optimizing language models for dialogue. *OpenAI blog*, 2(4), 2022.

[Sennrich *et al.*, 2016] Rico Sennrich, Barry Haddow, and Alexandra Birch. Neural machine translation of rare words with subword units. In *Proceedings of the 54th annual meeting of the association for computational linguistics (volume 1: long papers)*, pages 1715–1725, 2016.

[Su *et al.*, 2023] Yixuan Su, Tian Lan, Huayang Li, Jialu Xu, Yan Wang, and Deng Cai. Pandagpt: One model to instruction-follow them all. *arXiv preprint arXiv:2305.16355*, 2023.

[Sun *et al.*, 2023] Quan Sun, Qiyi Yu, Yufeng Cui, Fan Zhang, Xiaosong Zhang, Yueze Wang, Hongcheng Gao, Jingjing Liu, Tiejun Huang, and Xinlong Wang. Emu: Generative pretraining in multimodality. *arXiv preprint arXiv:2307.05222*, 2023.

[Team, 2024] Chameleon Team. Chameleon: Mixed-modal early-fusion foundation models. *arXiv preprint arXiv:2405.09818*, 2024.

[Vaswani *et al.*, 2017] Ashish Vaswani, Noam Shazeer, Niki Parmar, Jakob Uszkoreit, Llion Jones, Aidan N Gomez, Łukasz Kaiser, and Illia Polosukhin. Attention is all you need. *Advances in neural information processing systems*, 30, 2017.

[Wang *et al.*, 2024] Xinlong Wang, Xiaosong Zhang, Zhengxiong Luo, Quan Sun, Yufeng Cui, Jinsheng Wang, Fan Zhang, Yueze Wang, Zhen Li, Qiyi Yu, et al. Emu3: Next-token prediction is all you need. *arXiv preprint arXiv:2409.18869*, 2024.

[Wang *et al.*, 2025] Aowen Wang, Jiaqi Li, Hongyu Dong, Bocheng Xu, Qingyu Yin, Yanchao Xu, Jie Fu, and Junbo Zhao. Omnipred-gpt: a high-efficiency foundation model for comprehensive genomic sequence understanding. *Nature Communications*, 16(1):10139, 2025.

[Yang *et al.*, 2024] Xiaodong Yang, Guole Liu, Guihai Feng, Dechao Bu, Pengfei Wang, Jie Jiang, Shubai Chen, Qinmeng Yang, Hefan Miao, Yiyang Zhang, et al. Genecompass: deciphering universal gene regulatory mechanisms with a knowledge-informed cross-species foundation model. *Cell Research*, 34(12):830–845, 2024.

[Yang *et al.*, 2025] An Yang, Anfeng Li, Baosong Yang, Beichen Zhang, Binyuan Hui, Bo Zheng, Bowen Yu, Chang Gao, Chengen Huang, Chenxu Lv, et al. Qwen3 technical report. *arXiv preprint arXiv:2505.09388*, 2025.

[Zhai *et al.*, 2023] Xiaohua Zhai, Basil Mustafa, Alexander Kolesnikov, and Lucas Beyer. Sigmoid loss for language image pre-training. In *Proceedings of the IEEE/CVF international conference on computer vision*, pages 11975–11986, 2023.

[Zhang *et al.*, 2023a] Hang Zhang, Xin Li, and Lidong Bing. Video-llama: An instruction-tuned audio-visual language model for video understanding. *arXiv preprint arXiv:2306.02858*, 2023.

[Zhang *et al.*, 2023b] Xiaoman Zhang, Chaoyi Wu, Ziheng Zhao, Weixiong Lin, Ya Zhang, Yanfeng Wang, and Weidi Xie. Pmc-vqa: Visual instruction tuning for medical visual question answering. *arXiv preprint arXiv:2305.10415*, 2023.

[Zhang *et al.*, 2025] Xinjie Zhang, Jintao Guo, Shanshan Zhao, Minghao Fu, Lunhao Duan, Jiakui Hu, Yong Xien Chng, Guo-Hua Wang, Qing-Guo Chen, Zhao Xu, et al. Unified multimodal understanding and generation models: Advances, challenges, and opportunities. *arXiv preprint arXiv:2505.02567*, 2025.